JACS
JOURNAL OF THE AMERICAN CHEMICAL SOCIETY

COMMUNICATION

pubs.acs.org/JACS

Aqueous Cathode for Next-Generation Alkali-Ion Batteries

Yuhao Lu, John B. Goodenough,* and Youngsik Kim†

Texas Materials Institute, The University of Texas at Austin, Austin, Texas 78712, United States

Supporting Information

ABSTRACT: The lithium-ion batteries that ushered in the wireless revolution rely on electrode strategies that are being stretched to power electric vehicles. Low-cost, safe electrical-energy storage that enables better use of alternative energy sources (e.g., wind, solar, and nuclear) requires an alternative strategy. We report a demonstration of the feasibility of a battery having a thin, solid alkali-ion electrolyte separating a water-soluble redox couple as the cathode and lithium or sodium in a nonaqueous electrolyte as the anode. The cell operates without a catalyst and has high storage efficiency. The possibility of a flow-through mode for the cathode allows flexibility of the cell design for safe, large-capacity electrical-energy storage at an acceptable cost.

The appearance of lithium batteries with high power and energy density has triggered a revolution in the application of portable electronic devices and hybrid electric vehicles. Briefly, lithium batteries have experienced two generations since the concept was brought forth in 1958.[1] The commercialized primary lithium batteries of the 1970s can be considered as the first generation. The second generation of lithium batteries was developed as rechargeable lithium batteries. The state-of-the-art lithium batteries of the second generation focus on insertion compounds as cathode materials and carbon, carbon-buffered alloys, or oxides as anode materials.[2] Although intense effort has been devoted to the development of carbon or carbon-buffered alloys as anodes for lithium batteries, lithium metal still has the highest specific capacity (3860 mA h g^{-1}) and sodium metal would be cheaper; therefore, an important challenge for the third generation of alkali-ion batteries is how to fully and effectively utilize the high capacity of an alkali metal and increase the capacity of the cathode beyond what is possible with an insertion compound while operating at ambient temperature. The present sodium−sulfur battery operates above 300 °C.

Oxygen in air, an "inexhaustible resource" on earth, makes it possible to match the capacity of lithium metal. In theory, the specific energy of a lithium−oxygen (air) battery is 5200 W h kg^{-1}.[3] The high energy storage has stimulated a worldwide study of Li−air batteries.[4] A typical Li−air battery discharges at 2.5−2.7 V and charges at 4.2−4.4 V.[5] The large discrepancy of 1.7 V between the charge and discharge curves represents a low Coulombic efficiency (CE), even when expensive catalysts have been used to lower the overpotential of the oxygen reactions.[6] Moreover, slow oxygen diffusion in the cathode degrades the performance of the Li−air battery.

From the thermodynamic point of view, water can be directly used as the cathode in a lithium battery and demonstrates the overall reaction $Li + H_2O \rightarrow LiOH + \frac{1}{2}H_2(g)$. Since the 1970s, lithium−water batteries have been developed by several groups.[7] These lithium−water batteries operate below 2.0 V and are not rechargeable because of the evolution of H_2 in the $Li + H_2O$ reaction.

In theory, the decomposition potential of water is 4.27 V vs. Li/Li^+ at room temperature. The high theoretical potential predicts the possibility of obtaining a lithium−water battery with a high potential through a proper structural design. Recently, a Li|β-NiOOH (water) battery with an operating potential of ∼3.4 V was developed.[8] The cathode, β-NiOOH, exhibited a specific capacity of 256 mA h g^{-1}, but its capacity is still far smaller than that of lithium metal.

Here we present a new strategy for alkali-ion batteries using water-soluble redox couples as the cathode. The electrochemical reactions at the electrodes can be written as follows:

$$\text{anode}: \quad n\text{A} \rightarrow n\text{A}^+ + ne^-$$
$$\text{cathode}: \quad \text{M}^{z+}(\text{aq}) + ne^- \rightarrow \text{M}^{(z-n)+}(\text{aq})$$

where A = Li or Na, M represents a metal, and $1 \leq n < z$. The overall reaction is

$$n\text{A} + \text{M}^{z+}(\text{aq}) \rightarrow n\text{A}^+ + \text{M}^{(z-n)+}(\text{aq})$$

An aqueous cathode has a low viscosity and can be easily circulated in a flow-through configuration at room temperature. The aqueous cathode in the flow-through mode can be individually stored in a "fuel" tank, which reduces the volume of the battery and increases the design flexibility of the battery structure, as shown in Figure 1. Therefore, the A|M^{z+}(aq) battery has a specific energy high enough to challenge the high specific energies of fuel cells. A portable fuel-cell system can provide more than 10 times the energy density of a conventional lithium-ion rechargeable battery.[9] In flow-through mode, the aqueous electrode continuously passes through the cathode side of the A|M^{z+}(aq) battery to oxidize the alkali metal fully. The flow of the aqueous solution brings heat out of the battery system and keeps the battery working near ambient conditions. Unlike previous lithium−water batteries, the aqueous cathode is not plagued by H_2 evolution from the solution, and the battery is efficiently rechargeable. Moreover, a Na|M^{z+}(aq) battery would alleviate concerns about the availability of lithium.

Selection of the aqueous cathode is a key to the development of the A|M^{z+}(aq) battery. Aqueous electrodes must have the following characteristics: (1) proper redox potentials; (2) no side

Received: February 4, 2011
Published: March 28, 2011

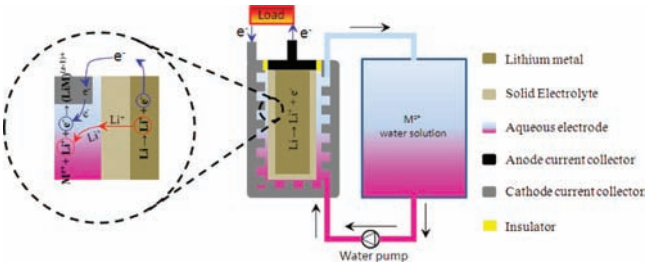

Figure 1. Example of a lithium−water rechargeable battery.

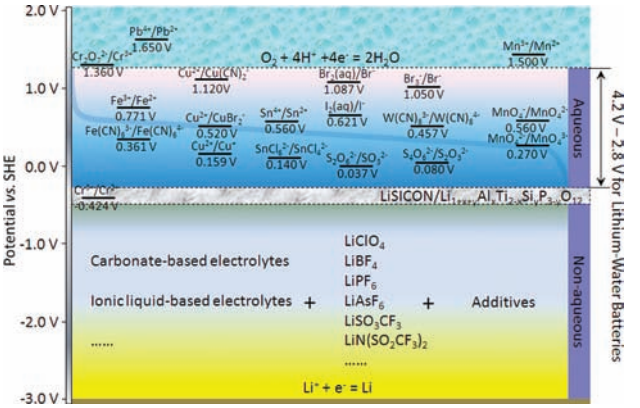

Figure 2. Systems for lithium−water batteries.

reactions; (3) good stability in water; (4) good reversibility; (5) reliable safety; and (6) low cost. Figure 2 shows possible systems for A|M^{z+}(aq) batteries (numerical values under the redox couples are their standard electrode potentials).[10] A second key element of an A|M^{z+}(aq) battery is a solid-electrolyte separator between the organic-liquid electrolyte on the anode side in contact with the solid A^0 and the aqueous cathode on the other side. An organic-liquid or polymer electrolyte must be used on the anode side to retain good anode−electrolyte contact during cycling as well as higher A^+-ion mobility. The dense A^+-ion solid-electrolyte separator must be thin and supported on a thick, porous, hydrophilic substrate. The solid electrolyte would block any dendrite growth of the A^0 anode from reaching the cathode, but this function means that the solid electrolyte should not be reduced by contact with A^0. Moreover, the solid electrolyte should probably present an oxide interface to the aqueous cathode. Development of a suitable solid electrolyte is still ongoing. Here we report a proof of concept with a relatively thick, commercially available lithium superionic conductor (LISICON), $Li_{1+x+y}Al_xTi_{2-x}Si_yP_{3-y}O_{12}$.[11]

In our initial proof-of-concept study, we used aqueous Fe$(NO_3)_3$/Fe$(NO_3)_2$ as the cathode.[12] The acidic character of this cathode attacked the Ti(IV) of the solid electrolyte, but the test proved promising. In a follow-up study, we used the $Fe(CN)_6^{3-}$/$Fe(CN)_6^{4-}$ couple in alkaline solution as the aqueous cathode. The stability of the commercial solid electrolyte (see Figure 4C and the Supporting Information) and water decomposition restricted our proof of concept with the commercial solid electrolyte to the voltage range 2.8 V < V < 4.2 V vs Li^+/Li (−0.2 to 1.2 V vs SHE). This restriction narrowed the range of cathode redox couples that could be selected from *Lange's Handbook*.[10] Since Sn ions are unstable in water solution and

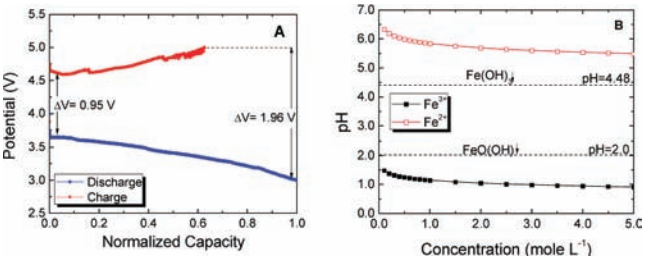

Figure 3. (A) Charge/discharge curves for the Li|Fe^{3+}(aq) battery. Cathode solution: 2 M Fe$(NO_3)_3$ + 1 M $LiNO_3$. Current: 0.5 mA. (B) Relationship between the Fe^{3+} and Fe^{2+} concentrations and the solution pH.

the Cr- and Pb-based redox couples lie outside the acceptable voltage range, we were left with Fe-, Cu-, and Mn-based redox couples. In the case of Cu- and Mn-based redox couples, side reactions either decreased the operating potential range or damaged the aqueous current collectors. Cu ions can be reduced to metallic Cu at a relatively high potential, which decreases the battery performance, and the reaction $MnO^{4-} + 2H_2O + 3e^- \rightarrow MnO_2(s) + 4OH^-$ takes place at 0.6 V vs SHE to stop the work of MnO_4^-/MnO_4^{2-} and MnO_4^{2-}/MnO_4^{3-}. The formation of the MnO_2 precipitate would destroy the reversibility of the battery. Other potential redox couples, such as $S_2O_6^{2-}$, I_2, and Br_2, have problems with toxicity and uncertain chemical properties in the lithium−water batteries. In this study, we focused on Fe-based redox couples. In Figure 2, Fe^{3+}/Fe^{2+} is located at 0.77 V vs SHE and $Fe(CN)_6^{3-}/Fe(CN)_6^{4-}$ at 0.36 V vs SHE, so the theoretical potential of a Li|Fe^{3+}(aq) battery is 3.77 V and that of a Li|$Fe(CN)_6^{3-}$(aq) battery is 3.40 V.

Figure 3A demonstrates the charge/discharge behavior of a Li|Fe^{3+}(aq) battery. Its open-circuit potential (OCP) was 3.99 V. When a current of 0.50 mA was applied to the battery, its potential initially dropped to 3.74 V. The discharge curve of the Li|Fe^{3+}(aq) battery slowly decreased with time to 3.00 V. The potential of the battery reached 4.73 V when it was charged following the discharge process. The ~1.0 V discrepancy between the discharge and charge curves suggests that the Li|Fe^{3+}(aq) battery shows relatively poor performance. Fe^{3+} is susceptible to hydrolysis in aqueous solution, and its solution is acidic, as shown in Figure 3B. According to its solubility-product constant, the pH of the solution depends on the Fe^{3+} concentration. When the Fe^{3+} solution concentration was 2 M, the solution pH was 1.1, but the solution pH changed to 5.7 when the Fe^{3+} was totally reduced to Fe^{2+} in the discharge process. The change in pH resulted in the formation of FeO(OH) (pH 2.0) and $Fe(OH)_3$ (pH 4.48) precipitates in the cathode solution. The precipitates not only decreased the active compound in the solution to lower the capacity but also covered the surface of the solid electrolyte to increase its resistance. After the first cycle, the capacity of the battery decreased to a very small value. Therefore, Fe^{3+}/Fe^{2+} should be excluded from the list of possible aqueous electrodes for lithium−water batteries.

The stability, solubility, and potential of $Fe(CN)_6^{3-}$/$Fe(CN)_6^{4-}$ bring hope to the development of a Li|aqueous cathode battery. According to the standard potential of $Fe(CN)_6^{3-}$/$Fe(CN)_6^{4-}$, the theoretical potential of the Li|$Fe(CN)_6^{3-}$(aq) battery is 3.40 V. Figure 4 demonstrates the electrochemical behavior of the Li|$Fe(CN)_6^{3-}$(aq) battery. The effective voltage of a typical Li|$Fe(CN)_6^{3-}$(aq) battery with the commercial solid

dx.doi.org/10.1021/ja201118f |*J. Am. Chem. Soc.* 2011, 133, 5756–5759

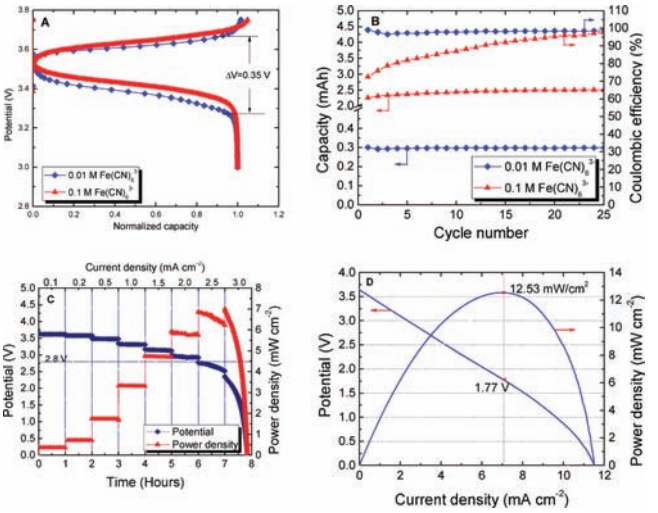

Figure 4. Electrochemical behavior of the Li|$Fe(CN)_6^{3-}$(aq) battery tested between 3.0 and 3.75 V. (A) Charge/discharge curves of the Li|$Fe(CN)_6^{3-}$ battery at the 20th cycle with different concentrations of the aqueous electrode. (B) Capacity retention and Coulombic efficiency for 20 cycles at a current density of 0.5 mA cm^{-2}. (C) Discharge behavior of the Li|$Fe(CN)_6^{3-}$ battery at different current densities. The aqueous electrode consisted of 1 M $K_3Fe(CN)_6$ + 0.5 M LiOH. (D) Polarization curve of the Li|$Fe(CN)_6^{3-}$ battery with a solution of 1 M $Fe(CN)_6^{3-}$ + 0.5 M LiOH.

electrolyte was between 3.33 and 3.68 V at a current of 0.5 mA cm^{-2}, as shown in Figure 4A. The change in the $Fe(CN)_6^{3-}$/$Fe(CN)_6^{4-}$ ratio led to the gradient in the charge/discharge curves. The gap between the discharge and charge curves of the Li|$Fe(CN)_6^{3-}$(aq) battery was far smaller than that of Li−air batteries. The concentrations of the redox couple in the aqueous electrode slightly affected the normalized discharge/charge curves. A concentration increase in the aqueous electrode from 0.01 to 0.1 M moved the curves up by ∼0.05 V; however, the concentration increase had a large effect on the capacity.

Unlike Li-insertion compounds and other solid electrodes, the charge/discharge processes of A|M^{z+}(aq) batteries did not cause a volume change of the cathode due to phase changes. Thus, the aqueous cathode demonstrated good reversibility, as shown in Figure 4B (Figure S1 shows the performance of the battery over 1000 cycles). In the present investigation, unflowed $K_3Fe(CN)_6$ solution was contained on the cathode side. The batteries presented good efficiencies. The battery with 0.01 M $Fe(CN)_6^{3-}$ solution showed a CE of 98.6% at the 25th cycle, and the CE in the battery with 0.1 M $Fe(CN)_6^{3-}$ solution was 97.6%.

Figure 4C shows the performance of a Li|$Fe(CN)_6^{3-}$(aq) battery at different current densities. In order to study the stability of the Li|$Fe(CN)_6^{3-}$(aq) battery, it was kept working at every current density for 1 h. When the current density was less than 2.5 mA cm^{-2}, the battery demonstrated a flat potential. Its performance became poor when the current density was larger than 2.5 mA cm^{-2} because of deterioration of the solid electrolyte below 2.8 V (see Figures S3C and S4). At a current density of 2.0 mA cm^{-2}, the power density of the battery was ∼5.9 mW cm^{-2}. Figure 4D shows a polarization curve for the Li|$Fe(CN)_6^{3-}$(aq) battery in a short time for the sake of the stability of the solid electrolyte (see Figure S3A,B). The battery can work safely at a power density of 12.53 mW cm^{-2} over a short time. Electrochemical reactions in the battery took place very rapidly, so kinetic polarization could not be observed at low current densities. The linear polarization curve in the low and medium current density ranges indicates that the performance of the battery was dominated by its resistance. In the high current density range, the abrupt drop in potential indicated a mass-transport loss due to the slow mobility of lithium ions in the solid electrolyte. Therefore, a decrease in the resistance of the solid electrolyte would dramatically improve the battery performance.

In conclusion, we have demonstrated the feasibility of an alkali-ion battery utilizing an alkali metal as the anode and a redox couple soluble in aqueous solution as the cathode. However, the capacity of an aqueous cathode is small, as noted in Figure 4B and Figure S1, requiring the concept to be extended to a flow-through mode for the cathode. Also, sodium rather than lithium might be used as the anode. This new strategy represents a third-generation alkali-ion battery promising lower cost than the conventional lithium-ion rechargeable battery, safe operation, and a Coulombic efficiency and voltage greater than those of a Li−air battery with, in principle, a comparable capacity. The demonstrated power output was limited by the commercially available solid electrolyte separating the organic-liquid or polymer anolyte and the aqueous cathode; the need for the design of a superior solid electrolyte has been indicated. The new strategy promises to be applicable to both the electric-vehicle market and the problem of electrical energy storage for the grid.

■ ASSOCIATED CONTENT

Supporting Information. Description of the Li|M^{z+}(aq) batteries used in the study, electrochemical testing methods, and more detailed experimental information. This material is available free of charge via the Internet at http://pubs.acs.org.

■ AUTHOR INFORMATION

Corresponding Author

jgoodenough@mail.utexas.edu

Present Addresses

[†]Department of Mechanical Engineering, Purdue School of Engineering and Technology, IUPUI, Indianapolis, IN 46202.

■ ACKNOWLEDGMENT

This work was supported by the Assistant Secretary for Energy Efficiency and Renewable Energy, Office of Vehicle Technologies, U.S. Department of Energy, under Contract DE-AC02-05CH11231 through the Batteries for Advanced Transportation Technologies (BATT) Program Subcontract 6805919. The work was also supported by the Office of Basic Energy Sciences, Office of Science, U.S. Department of Energy, under Contract DE-SC0005397. We thank Dr. Dawei Zhang for helpful discussions.

■ REFERENCES

(1) van Schalkwijk, W. A.; Scrosati, B. *Advances in Lithium-Ion Batteries*; Kluwer Academic Publishers: New York, 2002; pp 1−5.

(2) (a) Whittingham, M. S. *Chem. Rev.* **2004**, *104*, 4271. (b) Goodenough, J. B.; Kim, Y. *Chem. Mater.* **2010**, *22*, 587. (c) Tarascon, J.-M.; Armand, M. *Nature* **2001**, *414*, 359.

(3) Abraham, K. M.; Jiang, Z. *J. Electrochem. Soc.* **1996**, *143*, 1.

(4) Girishkumar, G.; McCloskey, B.; Luntz, A. C.; Swanson, S.; Wilcke, W. *J. Phys. Chem. Lett.* **2010**, *1*, 2193.

(5) Ogasawara, T.; Débart, A.; Holzapfel, M.; Novák, P.; Bruce, P. G. *J. Am. Chem. Soc.* **2006**, *128*, 1390.

(6) (a) Débart, A.; Bao, J.; Armstrong, G.; Bruce, P. G. *J. Power Sources* **2007**, *174*, 1177. (b) Lu, Y.-C.; Xu, Z.; Gasteiger, H. A.; Chen, S.; Hamad-Schifferli, K.; Shao-Horn, Y. *J. Am. Chem. Soc.* **2010**, *132*, 12170.

(7) (a) Littauer, E. L.; Tsai, K. C. *J. Electrochem. Soc.* **1976**, *123*, 771. (b) Shuster, N. *Proc. Int. Power Sources Symp., 34th* **1990**, 118. (c) Urquidi-Macdonald, M.; Flores, J.; Macdonald, D. D.; Pensado-Rodrguez, O.; Van Voorhis, D. *Electrochim. Acta* **1998**, *43*, 3069.(d) Shuster, N. Lithium−Water Battery. U.S. Patent 5,427,873, 1995.

(8) Li, H.; Wang, Y.; Na, H.; Liu, H.; Zhou, H. *J. Am. Chem. Soc.* **2009**, *131*, 15098.

(9) Service, R. F. *Science* **2002**, *292*, 1222.

(10) Speight, J. G. *Lange's Handbook of Chemistry*, 16th ed.; McGraw-Hill: New York, 2005; pp 1.380−1.395.

(11) Fu, J. Lithium Ion Conductive Glass-Ceramics. U.S. Patent 5,702,995, 1997.

(12) Goodenough, J. B.; Kim, Y. Presented at the 15th International Meeting on Lithium Batteries, Montréal, Canada, June 27−July 2, 2010.